Defining the clinical phenotype of Saul–Wilson syndrome

Carlos R. Ferreira, MD [1], Wadih M. Zein, MD[2], Laryssa A. Huryn, MD[2], Andrea Merker, PhD[3],
Seth I. Berger, MD, PhD[4], William G. Wilson, MD[5], George E. Tiller, MD, PhD[6],
Lynne A. Wolfe, MS, CRNP[7], Melissa Merideth, MD[7], Daniel R. Carvalho, MD, PhD[8],
Angela L. Duker, MS, CGC[9], Heiko Bratke, MD[10], Marte Gjøl Haug, MD[11], Luis Rohena, MD[12,13],
Hanne B. Hove, MD, PhD[14], Zhi-Jie Xia, PhD[15], Bobby G. Ng, BS[15], Hudson H. Freeze, PhD[15],
Melissa Gabriel, MS, CGC[16], Alvaro H. Serrano Russi, MD[16], Lauren Brick, MSc, CGC[17],
Mariya Kozenko, MD[17], Dawn L. Earl, ARNP[18], Emma Tham, MD, PhD[19,20], Gen Nishimura, MD[21],
John A. PhillipsIII, MD[22], William A. Gahl, MD, PhD[7], Rizwan Hamid, MD, PhD[22],
Andrew P. Jackson, MBBS, PhD[23], Giedre Grigelioniene, MD, PhD[19,20] and Michael B. Bober, MD, PhD[9]

Purpose: Four patients with Saul–Wilson syndrome were reported between 1982 and 1994, but no additional individuals were described until 2018, when the molecular etiology of the disease was elucidated. Hence, the clinical phenotype of the disease remains poorly defined. We address this shortcoming by providing a detailed characterization of its phenotype.

Methods: Retrospective chart reviews were performed and primary radiographs assessed for all 14 individuals. Four individuals underwent detailed ophthalmologic examination by the same physician. Two individuals underwent gynecologic evaluation. *Z*-scores for height, weight, head circumference and body mass index were calculated at different ages.

Results: All patients exhibited short stature, with sharp decline from the mean within the first months of life, and a final height *Z*-score between −4 and −8.5 standard deviations. The facial and radiographic features evolved over time. Intermittent neutropenia was frequently observed. Novel findings included elevation of liver transaminases, skeletal fragility, rod–cone dystrophy, and cystic macular changes.

Conclusions: Saul–Wilson syndrome presents a remarkably uniform phenotype, and the comprehensive description of our cohort allows for improved understanding of the long-term morbidity of the condition, establishment of follow-up recommendations for affected individuals, and documentation of the natural history into adulthood for comparison with treated patients, when therapeutics become available.

Genetics in Medicine (2020) https://doi.org/10.1038/s41436-019-0737-1

Keywords: Saul–Wilson syndrome; phenotype; COG4; G516R

INTRODUCTION

Saul–Wilson syndrome is a rare skeletal dysplasia originally described in 1982 in a child with bulging fontanelles, left clubfoot, severe short stature, blue sclerae, bilateral cataracts, blunted fingertips, and frequent otitis media with hearing loss.[1] In 1990, an update was provided on the original proband, and a second patient with similar features was reported,[2,3] while two additional affected individuals were described in 1994.[4] Recently, a recurrent de novo heterozygous COG4 amino acid substitution (p.Gly516Arg) was identified in 14 patients with the disease, including two of the four original individuals described in the 1990s.[5] COG4 is a component of the conserved oligomeric Golgi (COG) complex, a heterooctameric protein complex that regulates vesicular trafficking between the Golgi apparatus and the endoplasmic reticulum (ER). Patients' fibroblasts demonstrated accelerated retrograde Golgi-to-ER vesicular trafficking, while at the same time showing delayed anterograde

1

ER-to-Golgi trafficking, leading to disruption of the Golgi apparatus, with decreased volume and stack collapse. The glycosylation of a secreted proteoglycan, which normally takes place in the Golgi apparatus, was found to be impaired.[5]

Although the aforementioned work provides insight into the pathophysiology of the disease, a comprehensive clinical characterization of the phenotype is still needed. Our present work attempts to address this knowledge gap, as we provide an extensive description of the clinical phenotype of Saul–Wilson syndrome.

MATERIALS AND METHODS

Subjects
P1.1 was enrolled in protocol 15-HG-0130, "Clinical and Genetic Evaluation of Individuals with Undiagnosed Disorders Through the Undiagnosed Diseases Network" (NCT02450851).[6–8] P1.1, P2.1, P7.1, and P10.1 were enrolled in 14-HG-0071 "Clinical and Basic Investigations into Known and Suspected Congenital Disorders of Glycosylation" (NCT02089789). P3.1, P4.1, P5.1, P6.1, P9.1, P10.1, P11.1, P12.1, and P13.1 were enrolled in protocol 76-HG-0238, "Diagnosis and Treatment of Patients with Inborn Errors of Metabolism or other Genetic Disorders" (NCT00369421). The aforementioned protocols were approved by the National Human Genome Research Institute (NHGRI) Institutional Review Board (IRB). P3.1, P4.1, and P8.1 were enrolled in protocol "Enquiry of Participation in a Research Project about Clinical and Molecular Studies on Rare Congenital Skeletal Disorders," approved by the IRB of the Karolinska Institute in Sweden (2014/983–31/1). P2.1, P5.1, P5.2, and P7.1 were enrolled in the Primordial Registry at Nemours/Alfred I. duPont Hospital for Children, approved by the Nemours IRB. Written informed consent was obtained from all affected individuals or their parents/legal guardians; consent was also obtained for publication of patient photos, where appropriate. All 14 individuals were presented in a prior publication, focused on the molecular characterization of the disease.[5]

Data collection
Clinical and laboratory data were abstracted from the medical records by retrospective chart review. Further data were collected by direct interaction with participating individuals or their parents. Radiographic images were reviewed for all patients.

Ophthalmologic evaluation
Comprehensive age-appropriate eye evaluations were performed on four patients who visited the National Institutes of Health (NIH) Clinical Center. These included an evaluation of visual acuity, color vision, stereopsis, ocular motility assessment, mapping of visual fields with MonCV kinetic perimetry (Metrovision, Pérenchies, France), measurement of axial length (IOLMaster, Carl Zeiss Meditec, Dublin, CA), slit-lamp microscopy, dilated fundus exam, and retinoscopy to assess refractive error. Part of this assessment was performed at a sedated eye exam for P1.1. Ancillary testing,

when visit time and patient cooperation level allowed, included electroretinography with a UTAS console (LKC Technologies, Gaithersburg, MD) and Burian–Allen bipolar contact lens electrodes (Hansen Labs, Coralville, IA), color fundus photography (CFP), and fundus autofluorescence (FAF) imaging with Topcon (Topcon Medical Systems, Oakland, NJ), RetCAM3 (Clarity Medical System Inc., Pleasanton, CA), or Optos (Optos, Dunfermline, Scotland, UK) imaging systems, and Optical Coherence Tomography utilizing a Cirrus HD-OCT machine (Carl Zeiss Meditec, Dublin, CA).

Gynecologic evaluation
P2.1 and P7.1 underwent gynecologic evaluation through review of history and hormone testing for both patients and pelvic exam and pelvic ultrasound for one patient.

Growth
Growth data were available for 13 affected individuals. Growth parameters were corrected for gestational age. Individual growth parameters (height, weight, head circumference, and body mass index) were calculated at age groups selected a priori, as follows: birth, 3 months, 6 months, 9 months, 12 months, 18 months, 2 years, 3 years, 4 years, 5 years, 6 years, 7 years, and 8 years. Subsequently, mean, median, standard deviations, and Z-scores were calculated according to World Health Organization (WHO)[9,10] and UK90[11–13] references. For a graphic comparison of length/height to achondroplasia, stature reference from a European cohort was used.[14]

RESULTS
Clinical summaries for all patients are provided in the Supplementary Materials, Appendix 1.

Dysmorphic features
The characteristic facial features are depicted in Fig. 1 and Supplementary Fig. S1. During early infancy, patients have progeroid features that disappear within the first few months of life. Blue sclerae are also seen in early infancy, and can persist for several months. The scalp veins become particularly prominent in late infancy and during the toddler years. The columella becomes prominent during the first few years of life. In late childhood, the shape of the forehead, which was round in early childhood, becomes taller and less round. Short distal phalanges of the fingers and toes of variable severity are seen in all, regardless of age.

Ocular manifestations
The ocular manifestations of the four patients (P1.1, P2.1, P7.1, and P10.1) with comprehensive eye exams performed at the NIH Ophthalmic Genetics clinic are summarized in Supplementary Table S1 and documented in Fig. 2. All four had lamellar cataracts or a history of cataract extraction (with childhood-onset cataract). In addition, several whose ophthalmic histories were reviewed had progression of lamellar

cataracts requiring surgical intervention in early adulthood. Nystagmus was present in two of the four individuals who visited the NIH Clinical Center. The underlying cause is difficult to ascertain but is likely multifactorial with a central element. Two of the four individuals examined at the NIH Ophthalmic Genetics clinic had small eyes with short axial

Fig. 1 Phenotypic traits of patients with Saul–Wilson syndrome. (**a–d**) Progeroid features seen in the first few months of life: (**a**) P2.1, (**b**) P5.1, (**c**) P6.1, (**d**) P7.1. In addition, wrist contractures can be seen in (**a**), blue sclerae in (**a**) and (**d**), and boots and bar treatment for clubfoot in (**c**). (**e–h**) Facial features seen during early childhood: (**e**) P1.1, (**f**) P5.1, (**g**) P6.1, (**h**) P10.1. Note prominent, round forehead with prominent scalp veins in all. (**i–l**) Facial features seen in late childhood: (**i**) P7.1, (**j**) P5.1, (**k**) P6.1, (**l**) P10.1. The forehead is still prominent, but mainly tall rather than round. (**m,n**) Facial features in adolescence: (**m**) P2.1, (**n**) P7.1. (**o, p**) Facial features in adulthood (**o**) P2.1, (**p**) P7.1. (**q–t**) Feet in P1.1 at 4 years old (**q**), P9.1 at 9 years old (**r**), P7.1 at 27 years old (**s**), and P2.1 at 29 years old (**t**). Note short distal phalanges in all, and metatarsus varus in (**q**). (**u–x**) Hands in P1.1 at 4 years old (**u**), P4.1 at 5 years old (**v**), P9.1 at 9 years old (**w**), and P7.1 at 27 years old (**x**). Note short distal phalanges of variable degree in all.

length. Hyperopic refractive error was noted for these two patients as expected for short axial length; the other two had axial length within the normal range and were mildly myopic. A pigmentary retinopathy consistent with a rod–cone dystrophy was noted in all four patients, whereas macular cystic changes were documented in two of the four individuals seen at the NIH Clinical Center. Symptoms in this cohort include delayed dark adaptation, difficulty with night vision, and visual field deficits. Color vision can be affected with macular involvement. Although limited, our data indicated a trend toward progressively worse disease in older individuals; those specifically questioned indicated worsening of their night and peripheral vision with advancing age.

Gynecologic findings
Pubertal development was normal in both individuals (P2.1 and P7.1) undergoing gynecologic evaluation and age at menarche (12 years and 11.5 years) was similar to that of the general population.[15] Both began hormonal treatment (oral contraceptive pills or contraceptive patch) at age 16–17 years, one to manage menorrhagia and severe dysmenorrhea and the other to regulate her cycles and suppress ovarian cysts. One experienced elevated blood pressure on hormonal treatment, prompting discontinued use after 1 year. One underwent pelvic examination and pelvic ultrasound, which showed a normal-appearing uterus and ovaries that were small but likely proportionate to stature. Hormone levels (follicle-stimulating hormone [FSH], luteinizing hormone [LH], estradiol, testosterone, prolactin) were in the expected ranges for reproductive-age women. Although neither of the two adult females who underwent gynecologic evaluation has tried to conceive, regular menstrual cycles and a normal hormone profile suggest no impairment of the ability to conceive.

Growth
Table S2 demonstrates length/height, weight, head circumference, and body mass index as measured by standard deviation scores (corrected for gestational age) compared with the general population. Data are presented for individual patients, as well as mean and median for all available patients for the first eight years of life. Figure 3 presents standard deviation scores for length/height of individual patients compared with the general population; similar to what occurs in achondroplasia, there is a sharp decline in standard deviation scores during the first few months of life, with a final height between −4 and −8.5 SD scores.

Skeletal findings
Representative skeletal features are presented in Fig. 4 and Supplementary Fig. S2. Hypoplasia of the odontoid process, overtubulation of long bones with diaphyseal narrowing and metaphyseal flaring, and megaepiphyses are universal findings. Oval lucencies of the proximal femora are found during infancy. The vertebral bodies are initially flat, but become taller with age. The vertebral endplates become more irregular with age. Squared-off, ivory epiphyses of the hands are seen in later childhood. Several individuals had fractures (4/14, see Supplementary Fig. S3), in at least one case without any known trauma, and in other cases after minimal trauma. In addition, one had nonunion after surgical osteotomy (Supplementary Fig. S4). Premature degenerative joint disease was seen in two adults in their 20s, with early joint replacement in one (Supplementary Fig. S2J).

Laboratory findings
Asymptomatic elevation of transaminases was noticed in several individuals (Supplementary Fig. S5), without abnormalities in other liver function indices. Aspartate aminotransferase (AST) was elevated more often than alanine aminotransferase (ALT). Although neutropenia was not appreciated in any person when blood counts were obtained within the first two months of life ($n = 4$), it was noted in all individuals for whom values were available for analysis ($n = 12$). This neutropenia was intermittent, but did not have any noticeable cyclic periodicity. One (P10.1) was receiving chronic granulocyte colony stimulating factor (G-CSF) prophylaxis, with reported improvement of counts. Response to G-CSF in P13.1 was seen during an episode of orbital cellulitis, with a baseline absolute neutrophil count (ANC) of 1080 cells/μL, which improved to 1950 cells/μL after three daily doses of G-CSF at 5 mcg/kg/dose.

Misdiagnoses
Frequent misdiagnoses included Wiedemann–Rautenstrauch syndrome (with overlapping findings of early progeroid features, poor growth, frontal prominence with persistent opening of the anterior fontanelle, prominent scalp veins, a convex nasal ridge, and thin vermillion of the upper lip), Russell–Silver syndrome (considering the short stature, largely of prenatal onset with absence of postnatal catch-up growth, relative macrocephaly, large open fontanelle, blue sclerae, and ivory epiphyses), Hallermann–Streiff syndrome (given the short stature, cataracts, micrognathia, prominent scalp veins, and slender diaphyses), pycnodysostosis (given the short stature, persistently open fontanelle, short distal phalanges,
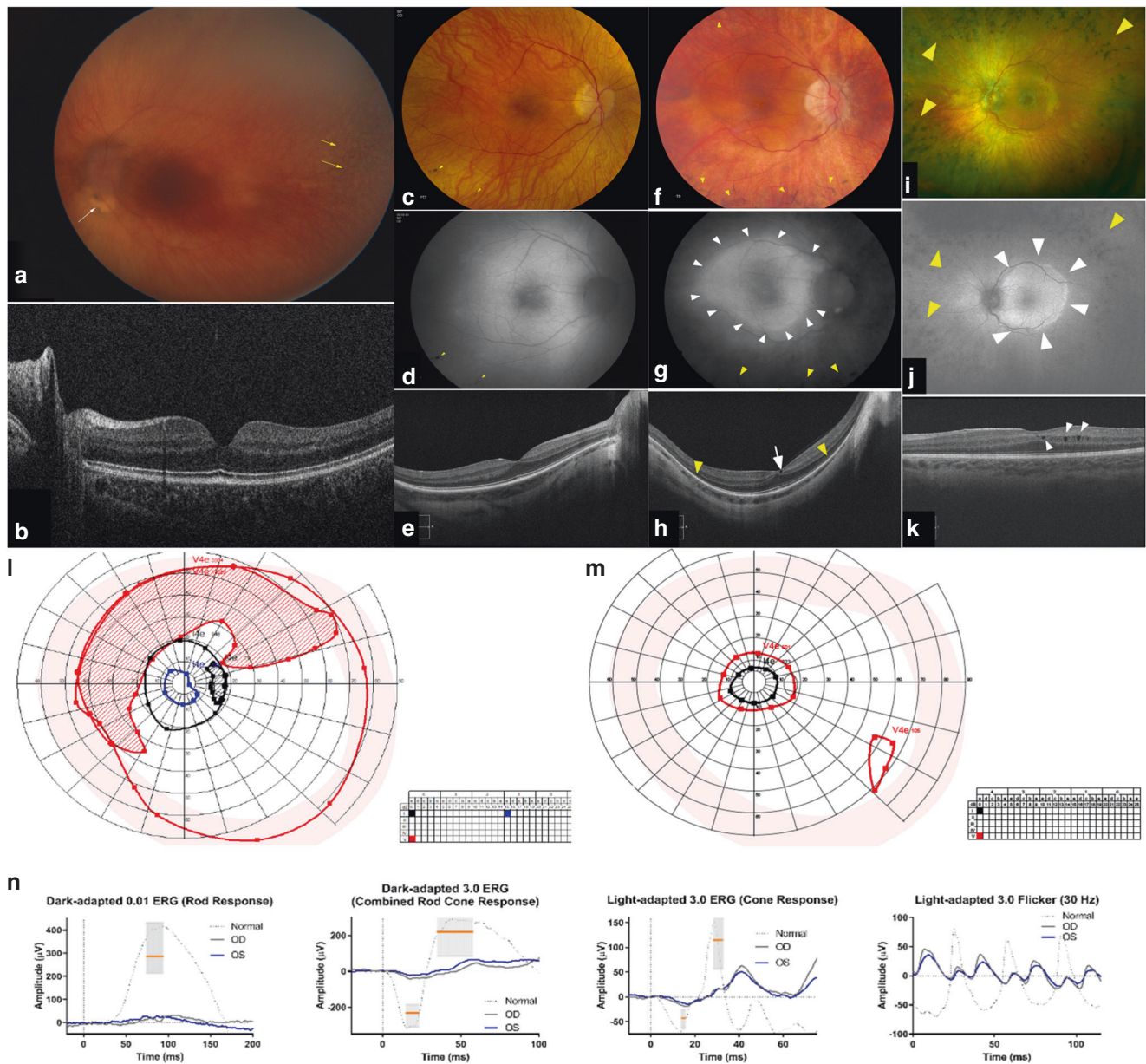
Fig. 2 Ophthalmologic findings. Clinical imaging of the ocular fundus, psychophysical testing, and electroretinography in individuals with Saul–Wilson syndrome. (**a**) Color fundus photography (CFP) of left eye of P1.1 obtained under anesthesia using a portable device (RetCam3) and showing mottling of the retinal pigment epithelium (yellow arrows) and an elevated lesion inferior to the optic nerve head (white arrow). Image clarity is reduced by the presence of lamellar cataract. (**b**) Bioptigen optical coherence tomography indicates preserved central retina including absence of macular cystic changes and normal ellipsoid zone (EZ) layer in P1.1. (**c, f**) CFP of the right and (**i**) left eye of affected individuals showing characteristic features of rod–cone dystrophies including attenuated retinal vessels, waxy pallor of optic nerve head, and midperipheral bony spicules (yellow arrowheads): (**c**) P2.1, (**f**) P7.1, (**i**) P10.1. (**d, g**) Fundus autofluorescence (FAF) images of the right eye and (**j**) left eye of affected individuals showing pigment deposition as hypoautofluorescence (yellow arrowheads) and a characteristic hyperautofluorescence ring (white arrowheads) typically seen in rod–cone dystrophies: (**d**) P2.1, (**g**) P:7.1, (**j**) P10.1. (**e, h**) Cirrus optical coherence tomography scans of the right eye and (**k**) left eye of affected individuals ranging from an almost normal scan in (**e**) to loss of ellipsoid zone EZ-band (yellow arrowheads) in (**h**) as well as presence of macular cystic changes in (**h, k**) (white arrowheads): (**e**) P2.1, (**h**) P7.1, (**k**) P10.1. (**l, m**) Kinetic perimetry of P2.1 and P7.1, respectively, showing different degrees of constriction and midperipheral scotomata. (**n**) Representative electroretinography (ERG) from P2.1 showing a reduction and delay of the scotopic responses to a greater degree than the photopic ones, confirming the presence of a rod–cone dystrophy.

and nonunion), osteogenesis imperfecta (due to blue sclerae, bone fragility, and hearing loss), and microcephalic osteodysplastic primordial dwarfism type II (due to profound short stature in most cases of prenatal onset, microcephaly, low hanging columella, thin bones with metaphyseal widening, metacarpal pseudoepiphyses, and ivory phalangeal epiphyses).

A summary of the most common clinical and imaging findings is presented in Fig. 5.
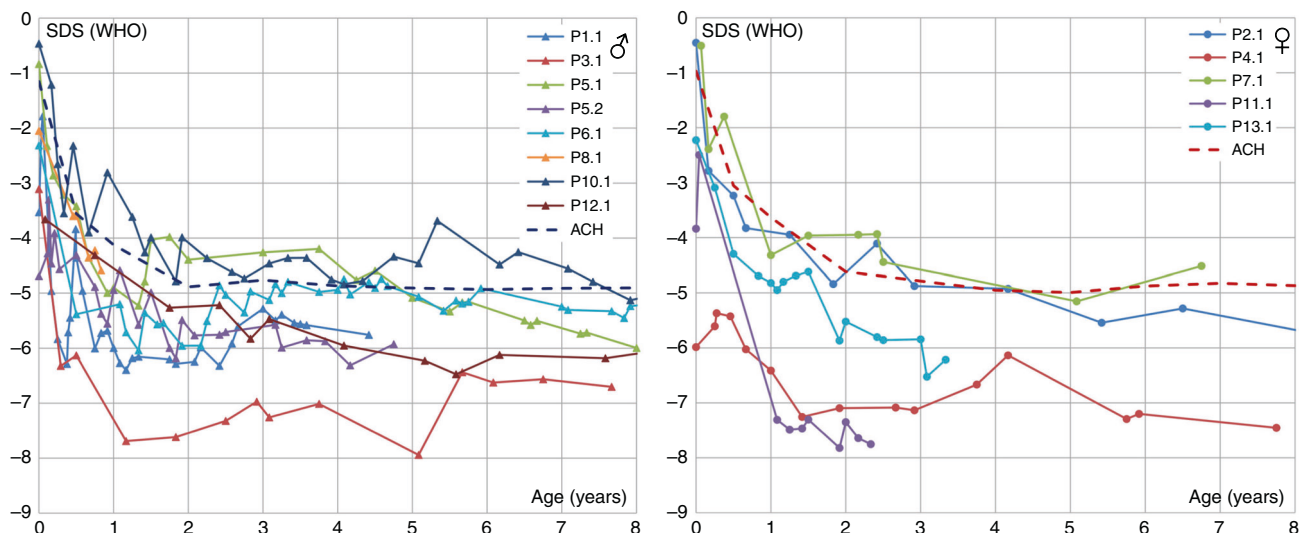
Fig. 3 Length/height expressed as standard deviation scores. Note a sharp decline in SD scores during the first few months of life, with an eventual plateau around −4 to −8.5 SD scores. Growth is near or below the mean stature for achondroplasia (dashed line). *WHO* World Health Organization.

DISCUSSION

Several age-dependent findings emanated from our study of the phenotype of an ultrarare disease, Saul–Wilson syndrome. First, although not all patients were born with weight or length more than 2 SD scores below the mean, all developed short stature within the first year of life, and none exhibited any catch-up growth. To put this into perspective, stature was generally lower than the mean for achondroplasia throughout their lifetimes. Second, most patients have a progeroid appearance during early infancy. The forehead is prominent throughout their lives, but is mainly round in early childhood, and becomes tall in late childhood. Blue sclerae are seen during the first few months to years of life, but then disappear. Third, neutropenia was not appreciated in the first two months of life, but was seen in all tested individuals subsequently. Fourth, the vertebral bodies become taller and the endplates irregular with age, while ivory epiphyses develop in late childhood. Short distal phalanges of fingers and toes were present from birth, and unlike other features, did not appear to change over time.

Bone abnormalities had at least two potential clinical consequences. First, the involvement of the epiphyses was a likely cause of osteoarticular pain in all three adult patients. In the case of P2.1, degenerative osteoarthritis was objectively diagnosed since her early 20s, radiographically and by direct observation at the time of surgery, leading to joint replacement on three occasions. P7.1 exhibited advanced degenerative changes of the left hip and decreased range of motion of the shoulder joints. Second, there is a suggestion of bone fragility, as four patients developed fractures, in at least one case with no known underlying trauma, and in another case with poor healing. An additional patient exhibited postsurgical nonunion, a finding also reported in the original proband in 1982,[1] who was not part of our cohort. Other disorders of vesicular trafficking are known to lead to bone fragility; these include SEC24D deficiency resulting in a syndromic form of

osteogenesis imperfecta (OMIM 616294),[16] and GORAB deficiency associated with geroderma osteodysplasticum (OMIM 231070).[17] Recently, a patient with juvenile osteoporosis and recurrent fractures was found to carry a de novo, heterozygous variant in *COPB2*,[18] encoding a β-subunit of the Golgi coatamer complex that has been shown to interact with different subunits of the COG complex.[19]

Several ocular manifestations are common in individuals with Saul–Wilson syndrome and require attention and specialized care for both the pediatric and adult patient. Lamellar cataracts appear to be common and are often noted early in childhood. Further investigation of the mechanism underlying the increased risk for cataractogenesis is required. Retinal degeneration consistent with a rod–cone dystrophy (retinitis pigmentosa) was present in all four patients who underwent detailed ophthalmic exams at the NIH Clinical Center; it was also reported in several patients whose records were reviewed. The exact mechanism for the occurrence of retinal degeneration in Saul–Wilson syndrome is not clear; however, other disorders of vesicular trafficking have been previously associated with retinal dystrophy, including Cohen syndrome[20,21] and deficiency of NBAS, a component of the SNARE complex.[22]

A novel finding in our investigation was elevation of transaminases, although liver failure did not develop in any patient. Other intracellular trafficking disorders have been associated with liver disease, including SCYL1 deficiency,[23] and deficiency of NBAS[24] and RINT1,[25] both subunits of the NRZ complex that participates in retrograde trafficking.[26] NBAS deficiency is also associated with bone fragility, presumably due to reduced collagen secretion,[27] while the recurrent liver disease is related to thermal susceptibility of the syntaxin 18 complex.[28] The latter finding is of particular interest, since different components of the COG complex interact with syntaxins,[19] while RINT1 interacts directly with the COG complex.[26]

Intermittent neutropenia was noted in all tested individuals. This might explain the patients' frequent respiratory infections in the first years of life, although the neutropenia persisted into adulthood while the number of respiratory infections decreased over time. Neutropenia is a complication of other disorders of intracellular trafficking, such as Cohen syndrome due to *VPS13B* disease-causing variants,[29] severe congenital neutropenia type 5 caused by *VPS45* variants,[30]

Fig. 4 Radiographs depicting skeletal features of individuals with Saul–Wilson syndrome. (**a–e**) Radiographs of lateral cervical spine in P4.1 at 8 months (**a**), P5.2 at 1 year 11 months (**b**), P3.1 at 2 years 6 months (**c**), P5.1 at 6 years 1 month (**d**), and P7.1 at 11 years 6 months (**e**). Note hypoplasia of the odontoid process in all (arrows). (**f–j**) Radiographs of lateral lumbar spine in P4.1 at 3 months old (**f**), P6.1 at 5 years 10 months (**g**), P5.1 at 6 years 7 months (**h**), P10.1 at 9 years 3 months (**i**), and P9.1 at 12 years 5 months (**j**). The vertebral bodies become taller and more irregular with age. Note hypoplasia of L1 in (**g**, **h**, **i**). (**k–o**) Radiographs of lower extremities in P7.1 at 23 days (**k**), P10.1 at 9 weeks (**l**), P8.1 at 6 months (**m**), P5.2 at 3 years 10 months (**n**), and P9.1 at 12 years 5 months (**o**). Note proximal femoral lucencies in the first few months of life (arrows), as well as overtubulation of the long bones with slender diaphyses and metaphyseal flaring in all. (**p–t**) Radiographs of hands in P4.1 at 3 months (**p**), P13.1 at 13 months (**q**), P6.1 at 6 years 9 months (**r**), P9.1 at 9 years 8 months (**s**), and P6.1 at 10 years (**t**). Note shortening of metacarpals and phalanges and cone-shaped epiphyses of the phalanges in all, accessory ossification centers of the proximal metacarpals (**q**, **r**, **t**), and the development of squared-off ivory epiphyses (arrows) in late childhood (**s**, **t**).
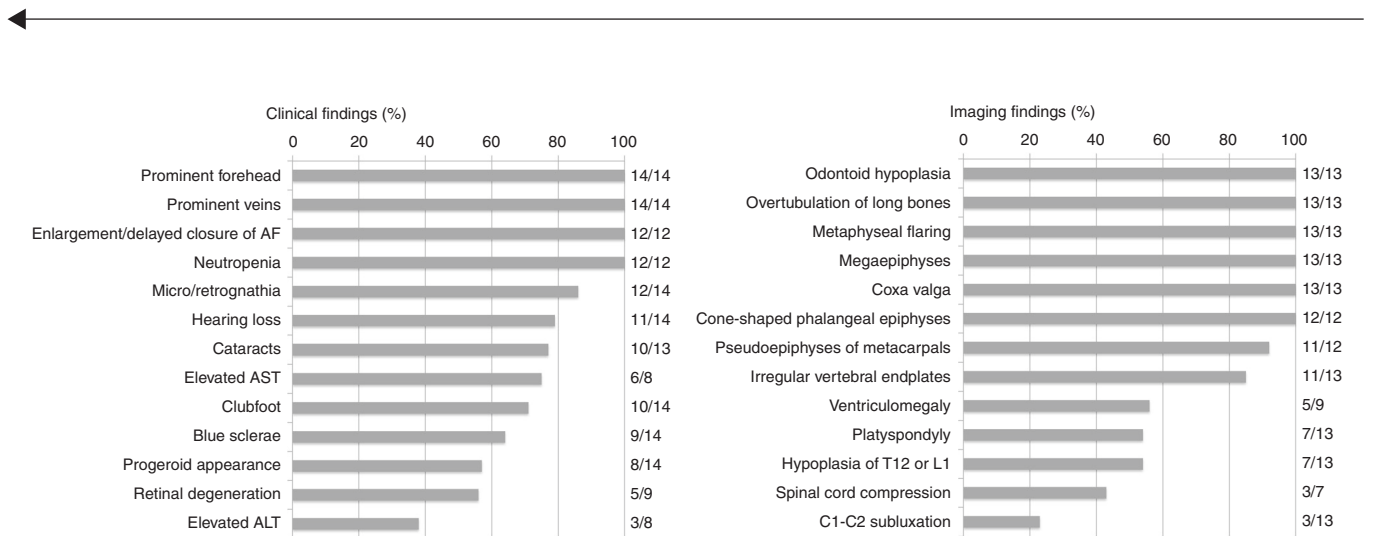

Fig. 5 Relative frequency of clinical and radiographic findings in Saul–Wilson syndrome. *AF* anterior fontanelle, *ALT* alanine aminotransferase, *AST* aspartate aminotransferase.

and adaptor protein complex 3 deficiency, causing Hermansky–Pudlak syndrome types 2 and 10;[31] in the latter disorders, the neutropenia is thought to be due to impaired intracellular trafficking of neutrophil elastase.[32] It is thus plausible that the neutropenia of Saul–Wilson syndrome could also be related to intracellular mislocalization of proteins.

Based on the identified complications of Saul–Wilson syndrome, we can begin to establish recommendations for clinical management. (1) Skeletal—odontoid hypoplasia and osteotomy considerations: Given the universal finding of odontoid hypoplasia, with frequent C1–C2 subluxation and/ or spinal cord compression, best practices in perioperative management of patients with skeletal dysplasias should be followed.[33] Skeletal surgery involving osteotomy should only be considered as a last resort, given poor healing and nonunion seen in a few patients. (2) Hearing—early evaluation and possible hearing aids: Since hearing loss represents a common complication, an audiologic evaluation should be performed at least yearly, or as frequently as recommended based on prior findings. Standard treatments for hearing loss (e.g., hearing aids) should be offered. (3) Ophthalmologic—cataracts and retinal degeneration: The presence of lamellar cataract needs to be assessed by a pediatric ophthalmologist and followed up for progression. If the cataract is dense enough to require surgery, this needs to be addressed to avoid the risk of amblyopia. Similarly, an

ophthalmologic evaluation for retinal degeneration is recommended on an annual basis. Standard treatments for cataracts and night blindness (e.g., night vision scopes, selected wavelength filters) should be offered. (4) Hematologic—neutropenia and possible G-CSF: In the setting of frequent infections, G-CSF prophylaxis should be considered, while acute infections in the setting of neutropenia can be managed by therapeutic G-CSF administration as needed. (5) Neurologic—hydrocephalus: Two patients underwent shunt placement for hydrocephalus. However, another patient with communicating hydrocephalus diagnosed in infancy had spontaneous resolution upon reimaging at 2 years of age. Thus, the possibility exists that individuals with Saul–Wilson syndrome might be predisposed to developing "benign external hydrocephalus," an entity associated with macrocephaly and increased volume of the subarachnoid space due to decreased absorption of the cerebrospinal fluid, with spontaneous resolution within the first few years of life.[34] It is unclear whether a conservative approach is indicated in most cases, but insertion of a shunt seems advisable for children showing signs of increased intracranial pressure. (6) Nutrition—gastrostomy: Three patients underwent gastrostomy tube insertion. This likely represents an attempt by well-intended physicians to improve the child's growth; however, overfeeding should be avoided. (7) Genetic counseling: Although most individuals show de novo inheritance of the pathogenic variant, sib recurrence was observed in one family (1/13),

probably due to germline mosaicism in a parent; thus, the recurrence risk in siblings of a proband is greater than that of the general population.

In summary, we have carefully delineated the phenotype of Saul–Wilson syndrome, providing improved understanding of the morbidity of the disease and allowing for better surveillance and management of affected individuals.

SUPPLEMENTARY INFORMATION

The online version of this article (https://doi.org/10.1038/s41436-019-0737-1) contains supplementary material, which is available to authorized users.

DISCLOSURE

The authors declare no conflicts of interest.

Publisher's note Springer Nature remains neutral with regard to jurisdictional claims in published maps and institutional affiliations.

REFERENCES

1. Saul RA. Unknown cases. Proc Greenwood Genet Center. 1982;1:102–105.
2. Saul RA, Wilson WGA. "New" skeletal dysplasia in two unrelated boys. Am J Med Genet. 1990;35:388–393.
3. Saul RA, Wilson WGA. COMMENTARY—the Saul–Wilson syndrome from its early days until now. Am J Med Genet A. 2019;179:159–160.
4. Hersh JH, Joyce MR, Spranger J, et al. Microcephalic osteodysplastic dysplasia. Am J Med Genet. 1994;51:194–199.
5. Ferreira CR, Xia Z-J, Clément A, et al. A recurrent de novo heterozygous COG4 substitution leads to Saul–Wilson syndrome, disrupted vesicular trafficking, and altered proteoglycan glycosylation. Am J Hum Genet. 2018;103:553–567.
6. Gahl WA, Wise AL, Ashley EA. The Undiagnosed Diseases Network of the National Institutes of Health: a national extension. JAMA. 2015;314:1797–1798.
7. Gahl WA, Mulvihill JJ, Toro C, et al. The NIH Undiagnosed Diseases Program and Network: applications to modern medicine. Mol Genet Metab. 2016;117:393–400.
8. Ramoni RB, Mulvihill JJ, Adams DR, et al. The Undiagnosed Diseases Network: accelerating discovery about health and disease. Am J Hum Genet. 2017;100:185–192.
9. WHO Multicentre Growth Reference Study Group. WHO child growth standards: length/height-for-age, weight-for-age, weight-for-length, weight-for-height and body mass index-for-age: methods and development. Geneva: World Health Organization; 2006. https://www.who.int/childgrowth/standards/velocity/technical_report/en/. Accessed 13 Nov 2019.
10. WHO Multicentre Growth Reference Study Group. WHO child growth standards: growth velocity based on weight, length and head circumference: methods and development. Geneva: World Health Organization; 2009. https://www.who.int/childgrowth/standards/technical_report/en/. Accessed 13 Nov 2019.
11. Cole TJ, Green PJ. Smoothing reference centile curves: the LMS method and penalized likelihood. Stat Med. 1992;11:1305–1319.
12. Freeman JV, Cole TJ, Chinn S, Jones PR, White EM, Preece MA. Cross sectional stature and weight reference curves for the UK, 1990. Arch Dis Child. 1995;73:17–24.
13. Cole TJ, Freeman JV, Preece MA. British 1990 growth reference centiles for weight, height, body mass index and head circumference fitted by maximum penalized likelihood. Stat Med. 1998;17:407–429.
14. Merker A, Neumeyer L, Hertel NT, et al. Growth in achondroplasia: development of height, weight, head circumference, and body mass index in a European cohort. Am J Med Genet A. 2018;176:1723–1734.
15. McDowell MA, Brody DJ, Hughes JP. Has age at menarche changed? Results from the National Health and Nutrition Examination Survey (NHANES) 1999-2004. J Adolesc Health. 2007;40:227–231.
16. Garbes L, Kim K, Rieß A, et al. Mutations in SEC24D, encoding a component of the COPII machinery, cause a syndromic form of osteogenesis imperfecta. Am J Hum Genet. 2015;96:432–439.
17. Hennies HC, Kornak U, Zhang H, et al. Gerodermia osteodysplastica is caused by mutations in SCYL1BP1, a Rab-6 interacting golgin. Nat Genet. 2008;40:1410–1412.
18. Marom R, Burrage LC, Jain M, et al. COPB2 loss of function leads to disrupted collagen trafficking and juvenile osteoporosis. J Bone and Miner Res. 2018;33(S1):76.
19. Willett R, Ungar D, Lupashin V. The Golgi puppet master: COG complex at center stage of membrane trafficking interactions. Histochem Cell Biol. 2013;140:271–283.
20. Kivitie-Kallio S, Summanen P, Raitta C, Norio R. Ophthalmologic findings in Cohen syndrome. A long-term follow-up. Ophthalmology. 2000;107:1737–1745.
21. Chandler KE, Biswas S, Lloyd IC, Parry N, Clayton-Smith J, Black GCM. The ophthalmic findings in Cohen syndrome. Br J Ophthalmol. 2002;86:1395–1398.
22. Segarra NG, Ballhausen D, Crawford H, et al. NBAS mutations cause a multisystem disorder involving bone, connective tissue, liver, immune system, and retina. Am J Med Genet A. 2015;167A:2902–2912.
23. Lenz D, McClean P, Kansu A, et al. SCYL1 variants cause a syndrome with low γ-glutamyl-transferase cholestasis, acute liver failure, and neurodegeneration (CALFAN). Genet Med. 2018;20:1255–1265.
24. Haack TB, Staufner C, Köpke MG, et al. Biallelic mutations in NBAS cause recurrent acute liver failure with onset in infancy. Am J Hum Genet. 2015;97:163–169.
25. Cousin MA, Conboy E, Wang J-S, et al. RINT1 bi-allelic variations cause infantile-onset recurrent acute liver failure and skeletal abnormalities. Am J Hum Genet. 2019;105:108–121.
26. Tagaya M, Arasaki K, Inoue H, Kimura H. Moonlighting functions of the NRZ (mammalian Dsl1) complex. Front Cell Dev Biol. 2014;2:25.
27. Balasubramanian M, Hurst J, Brown S, et al. Compound heterozygous variants in NBAS as a cause of atypical osteogenesis imperfecta. Bone. 2017;94:65–74.
28. Staufner C, Haack TB, Köpke MG, et al. Recurrent acute liver failure due to NBAS deficiency: phenotypic spectrum, disease mechanisms, and therapeutic concepts. J Inherit Metab Dis. 2016;39:3–16.
29. Kolehmainen J, Black GCM, Saarinen A, et al. Cohen syndrome is caused by mutations in a novel gene, COH1, encoding a transmembrane protein with a presumed role in vesicle-mediated sorting and intracellular protein transport. Am J Hum Genet. 2003;72:1359–1369.
30. Vilboux T, Lev A, Malicdan MCV, et al. A congenital neutrophil defect syndrome associated with mutations in VPS45. N Engl J Med. 2013;369:54–65.

31. Ammann S, Schulz A, Krägeloh-Mann I, et al. Mutations in AP3D1 associated with immunodeficiency and seizures define a new type of Hermansky–Pudlak syndrome. Blood. 2016;127:997–1006.

32. Benson KF, Li F-Q, Person RE, et al. Mutations associated with neutropenia in dogs and humans disrupt intracellular transport of neutrophil elastase. Nat Genet. 2003;35:90–96.

33. White KK, Bompadre V, Goldberg MJ, et al. Best practices in perioperative management of patients with skeletal dysplasias. Am J Med Genet A. 2017;173:2584–2595.

34. Zahl SM, Egge A, Helseth E, Wester K. Benign external hydrocephalus: a review, with emphasis on management. Neurosurg Rev. 2011;34:417–432.